

Interaction of an Oscillating Control Surface with an Unsteady Separated Region

James D. Lang* and M.S. Francis†

U.S. Air Force Academy, Colo.

The results of experiments involving an airfoil with an oscillating fence-type spoiler are utilized in the development of a semiempirical flow model capable of describing the surface effects of a dynamically separating region. Founded on an extension of steady flow separation concepts, the model incorporates a prediction of growth lag and modifications to the pressure field of the separation "bubble" as its essential features. The model is employed in the equation of motion for a system involving a mechanically and aerodynamically coupled spoiler/control surface combination undergoing oscillations. Resultant system behavior was predicted adequately, as verified by subsequent experiments. Limit cycle motion, which may be thought of as a subsonic analog of control surface buzz, was observed to correlate with analytical estimates.

Nomenclature

A	= control surface moment of inertia about the hinge-line
A_b	= cross-sectional area of separation bubble at airfoil centerline
a	= slope of a linear velocity profile
B	= mechanical damping of control surface
b	= airfoil and control surface span
C	= structural stiffness of control surface
C_H	= nondimensional hinge-moment coefficient, $C_H = H / (q_\infty b c_f^2)$
$C_{H_\beta}, C_{H_{\dot{\beta}}}$	= nondimensional derivatives, e.g., $C_{H_\beta} (U_\infty / c_f) \partial C_H / \partial \beta$
$> C_H$	= hinge-moment coefficient due to spoiler-induced loading
C_p	= pressure difference coefficient, non-dimensionalized by freestream dynamic pressure
c, c_f	= airfoil and control surface chord, respectively
E	= ratio of bubble length to spoiler height, assumed constant in steady flow
H	= control surface hinge-moment
$H_\beta, H_{\dot{\beta}}$	= dimensional partial derivatives, e.g., $H_\beta = \partial H / \partial \beta$
ΔH	= hinge-moment due to spoiler-induced loading
h_s, h	= actual and nondimensional spoiler height, $h = h_s / c_f$
$h_0, \Delta h$	= nondimensional mean spoiler height and amplitude
h_{01}	= mean spoiler height for zero control surface deflection for the coupled configuration
k	= control surface/spoiler mechanical coupling parameter
k_i	= bubble or shear layer shape factors, $i = 1, 2, 3$
ℓ_s, ℓ	= actual and nondimensional bubble length, measured from spoiler to reattachment location
$\dot{m}_{in}, \dot{m}_{out}$	= mass flow rates per unit span in and out of the separated region
\dot{m}_e	= hypothetical mass flow rate per unit span in unsteady flow
p	= surface static pressure
q_∞	= freestream dynamic pressure, $q_\infty = \frac{1}{2} \rho U_\infty^2$

U	= x-component of mean velocity at edge of shear layer
U_∞	= freestream velocity
u	= x-component of mean velocity
x	= chordwise distance measured from spoiler location
y	= distance measured normal to airfoil surface
β	= control surface deflection angle, positive trailing edge down
$\beta_0, \Delta \beta$	= center and amplitude of control surface oscillation
δ	= shear-layer thickness
κ	= constant, $\kappa \equiv (q_\infty b c_f^2) / A$
λ	= damping parameter, $\lambda \equiv \Delta \dot{\beta} / \Delta \beta$
ρ	= freestream density
ϕ	= phase angle relating control-surface deflection to spoiler motion
ψ	= phase angle relating hinge-moment coefficient to spoiler motion
ω	= angular frequency of oscillation
\tilde{z}	= perturbation to quantity z
\dot{z}	= time derivative of quantity z

Subscripts

b	= chordwise location where mixing and reattachment begins
n	= coefficient of n th term in a series
o	= mean value
r	= chordwise location of reattachment
s	= chordwise location of separation at spoiler

Introduction

FLOW separation and reattachment are physical phenomena that can be expected to exist and must be confronted in a wide variety of engineering problems. They frequently pose the most serious obstacle toward the attainment of a satisfactory quantitative prediction of the overall flowfield because of the complexity of the interaction of the governing physical mechanisms. This is even more evident when the flow under consideration is unsteady.

Complete quantitative analysis is, in general, unattainable through simple mathematical means but may be achieved through extensive numerical techniques. Modeling of the separated region by methods that are mathematically less rigorous but physically justified does, however, afford an appealing approach to the problem. Problems in aerodynamics which involve an interaction between a separating flow and an adjacent surface and which may be analyzed by this method

Received June 9, 1975; presented as Paper 75-867 at the AIAA Fluid and Plasma Dynamics Conference, Hartford, Conn., June 16-18, 1975; revision received Jan. 19, 1975. This research was sponsored by the Frank J. Seiler Research Laboratory,

Index category: Nonsteady Aerodynamics.

*Major, USAF. Associate Professor, Department of Aeronautics. Member AIAA.

†ILT, USAF. Research Associate, Frank J. Seiler Research Laboratory.

include those of control surface buzz and dynamic stall, to name two.

The research described in this paper is concerned with a related problem that involves the effects of a dynamically separating region on an adjacent control surface. A separation zone is created behind an oscillating fence-type spoiler located at midchord on the upper surface of an airfoil in subsonic flow. The primary advantage of the configuration is that of positive controllability of the separation point for this region. The behavior of a plain flap-type control surface located at the trailing edge is examined with respect to the induced unsteady loading generated by separation.

Numerous investigators have chronicled their research efforts in the study of separated flows. An excellent survey of the progress in this area is found in Chang's book.¹ Other important contributions in the study of separated flows can be found, for example: 1) in the analytical work of Crimi and Reeves² which deals with a separated laminar shear layer that transitions to a turbulent shear layer prior to reattachment onto a surface; 2) in the experimental study of Newman³ which considers a separated region aft of a fence-type spoiler; 3) in the analytical work of Norbury and Crabtree⁴ which examines the mixing and reattachment region of a steady separation bubble; and 4) in a study by Horton⁵ which is concerned with growth and bursting of laminar leading edge separation bubbles.

Trilling⁶ has offered a model of a separated region in which considerations of unsteady mass flux are employed in the determination of its growth characteristics in unsteady flow.

The research described herein seeks to develop a semiempirical model of the unsteady "bubble" in that it is based on the outcome of several preliminary experiments and relies on an extension of steady flow concepts. Detailed aspects of the model were applied to the analysis of the motion of a mechanically (as well as aerodynamically) coupled spoiler and control surface combination. Subsequent experiments duplicating this configuration were employed to verify the analytical results.

Steady Flow Separation Bubble

A large-scale separated region of so-called dead air is a common characteristic in many flowfields. Flow over tall forward- or rearward-facing steps and over tall fence-type spoilers, as in the present study, involves long separation bubbles which can be defined geometrically by points of separation s and reattachment r , as in Fig. 1. As discussed by Barnes⁷ and Chang,¹ a long, nominally two-dimensional separation bubble in steady flow has at least the following general features:

- 1) It has a near-constant ratio ℓ_s/h_s , which is weakly dependent on Reynolds number based on the boundary-layer thickness and velocity at the separation point location in the absence of the spoiler. The ratio may be strongly dependent on end-plate (i.e., three-dimensional flow) conditions.
- 2) It has a surface pressure distribution from s to r which may be approximated by a "rooftop" shape, as shown in Fig. 2, where $C_p \equiv (p - p_0)/(\rho U_\infty^2/2)$. C_p is a pressure coefficient referenced to pressures in the absence of a step or spoiler. It is nearly a constant in the forward portion of the dead air region from s to b and is approximately independent of step or spoiler height h_s . The rooftop distribution includes a linear

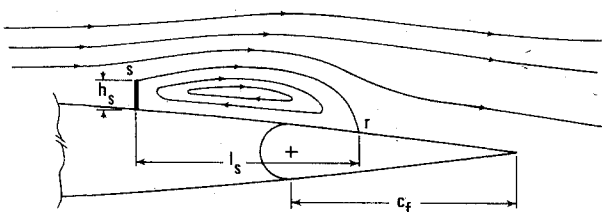


Fig. 1 Airfoil configuration and flow geometry.

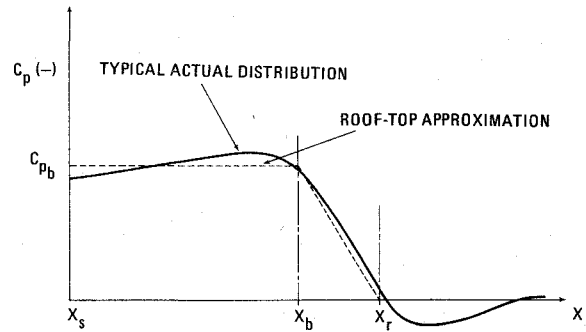


Fig. 2 Surface pressure distributions.

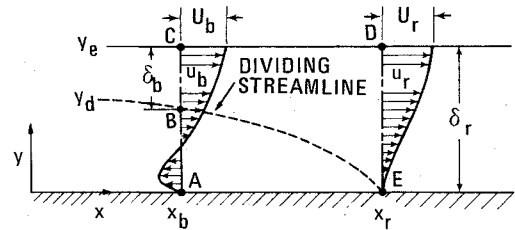


Fig. 3 Mean velocity profiles near reattachment.

pressure recovery in a mixing and reattachment region beginning at b , to a value near zero at reattachment.

3) It exhibits an interior region below the mean dividing streamline which involves slowly recirculation fluid. Circulation is maintained, in part, by the action of shear stresses that are at a maximum value near the dividing streamline.

Modeling of a steady flow bubble requires incorporation of the preceding features; for example, the ratio ℓ/h is defined as

$$\ell/h \equiv E = \ell_s/h_s \quad (1)$$

where ℓ and h are nondimensional heights based on control surface chord. Bubble area A_b may be represented as

$$A_b = k_1 h \ell = k_1 E h^2 \quad (2)$$

where k_1 is a constant that may be viewed as a geometric shape factor.

In addition, Norbury and Crabtree⁴ have shown that the pressure rise across the bubble (from b to r) can be related to shear layer parameters at b and r through an integral form of the momentum equation; that is,

$$\frac{p_b - p_r}{\frac{1}{2} \rho U_\infty^2} \approx C_{pb} = \frac{2}{\delta_r U_\infty^2} \left[U_r^2 (\delta_r - \theta_r - \delta_r^*) - \frac{1}{3} u_b^2 \delta_b \left(1 + \frac{1}{a} + \frac{1}{a^2} \right) \right] \quad (3)$$

where U_r , δ_r , and δ_b are defined in Fig. 3.

In Fig. 3, y_e represents the outer edge of the shear layer, and y_d the dividing streamline. A linear velocity profile between points B and C is assumed, with the velocity at B , u_b , determined by:

$$u_b = a U_b$$

θ_r and δ_r^* are the momentum and displacement thicknesses of the shear layer at reattachment. p_b and p_r are pressures, assumed uniform in a direction normal to the surface, at stations b and r , respectively.

Extension of Steady Flow Model to Unsteady Flow

The foregoing description of the separation bubble is applied readily to the case of an airfoil with a fixed spoiler on

one surface. These concepts can be extended to the case of spoiler oscillations with certain restrictions as follows.

With the spoiler forced to oscillate sinusoidally with small amplitude about a mean position, we can write $h(t) = h_0 + \tilde{h}(t)$, where $\tilde{h}(t) = \Delta h \cos \omega t$, and $\Delta h/h_0 < 1$. If the separated region grew in a quasisteady manner in unsteady flow, then an unsteady mass flux can be identified by applying an integral form of the continuity equation to the bubble interior:

$$\rho [d(A_b)/dt] = \dot{m}_e(t)$$

Upon differentiating Eq. (2), we further find that the assumed mass flux \dot{m}_e is related to spoiler mean height and rate of motion by a first-order approximation

$$\frac{d(A_b)}{dt} = \frac{d(k_1 E h^2)}{dt} = 2k_1 E h \dot{h} \approx 2k_1 E h_0 \dot{\tilde{h}}$$

where the parameters k_1 and E are assumed time invariant to first order. The mass flux term is therefore

$$\dot{m}_e(t) \approx \rho 2k_1 E h_0 \dot{\tilde{h}}(t) \quad (4)$$

Quasisteady bubble growth would involve bubble length perturbations that are in phase with spoiler height. In Ref. 6, Trilling argues that, since a characteristic time for the outer shear layer (i.e., the portion of the shear layer external to the mean dividing streamline) is δ/U_∞ as compared to $\ell_s/|U_c|$ for the separated region (where U_c is a characteristic mean velocity in the bubble interior), an appropriate assumption is that the outer shear layer reacts instantaneously to spoiler motion in incompressible flow.

The mass flux relation, Eq. (4), can be used in conjunction with the quasisteady assumption on the outer shear layer and Eq. (3), the pressure rise relation, to find perturbations to the pressure at station b . It is assumed further that shear layer parameters near the reattachment point, such as pressure, thickness, and velocities, are not affected significantly in unsteady flow and that the fluid represented by the mass flux \dot{m}_e enters (or leaves) the separated region near the dividing streamline between stations b and r .

Under these assumptions, the mass flux term \dot{m}_e can be related to the velocity at point B , u_B , and a perturbation to the "dividing streamline" location, δ_b :

$$\dot{m}_e = -\rho u_B \tilde{\delta}_b$$

The (quasi) steady flow continuity equation applied to the section BC yields

$$u_B \tilde{\delta}_b = -\tilde{u}_B \delta_b$$

Thus, perturbations to the pressure p_b involve changes only to the assumed velocity field parameter $u_b(y)$ and δ_b . Equation (3) can be used to solve for the resultant perturbation to C_{pb} ; i.e.,

$$\begin{aligned} \tilde{C}_{pb} &\approx \frac{-2}{\delta_r U_\infty^2} \left[\frac{1}{3} \left(1 + \frac{1}{a} + \frac{1}{a^2} \right) + 1 \right] u_B \frac{\dot{m}_e}{\rho} \\ &= \frac{-2u_B \dot{m}_e}{\rho U_\infty^2 \delta_r} \left[\frac{1}{3} \left(4 + \frac{1}{a} + \frac{1}{a^2} \right) \right] \end{aligned} \quad (5)$$

Note that Eq. (5) contains a term that accounts for a change of momentum flux near the dividing streamline which must take place to allow fluid to enter or leave the bubble.

A unique feature, then, of the unsteady separated region is that the interior pressure field is perturbed in unsteady flow. That this perturbation is related to spoiler rate of motion can be seen by combining Eqs. (4) and (5) to yield

$$\tilde{C}_{pb} \approx \frac{-4u_B k_1 E h_0}{U_\infty^2 \delta_r} \left[\frac{1}{3} \left(4 + \frac{1}{a} + \frac{1}{a^2} \right) \right] \dot{\tilde{h}}(t)$$

Also, it is assumed that shear layer thickness at reattachment is related linearly to mean spoiler height so that $h_0/\delta_r \approx h_0/\delta_{r0} = \text{const}$. The characteristic mean flow velocity U_c is introduced, along with the assumption that $u_B/|U_c| = \text{const}$, and we have

$$\tilde{C}_{pb} \approx -k_2 (c_f/U_\infty) |U_c/U_\infty| \dot{\tilde{h}}(t)$$

where

$$k_2 = \frac{k_1 E h_0 u_B}{c_f \delta_{r0} |U_c|} \left[\frac{4}{3} \left(4 + \frac{1}{a} + \frac{1}{a^2} \right) \right]$$

Since $\dot{\tilde{h}}(t) = -\omega \Delta h \sin \omega t$, we have the final expression

$$\tilde{C}_{pb} \approx k_2 |U_c/U_\infty| \nu \Delta h \sin \omega t \quad (6)$$

where the reduced frequency parameter ν is defined as follows:

$$\nu \equiv \omega c_f / U_\infty$$

A second feature of the model for unsteady flow follows from the work of Trilling⁶ and East and Wilkinson,⁸ who recognized the importance of convection of mass into the separated region and its relationship to the size of the region. The approach taken here is to consider again an integral form of the continuity equation applied to the bubble interior:

$$\rho [d(A_b)/dt] = \dot{m}_{in} - \dot{m}_{out}$$

and assume that the parameters governing bubble shape (spoiler height h and length of bubble ℓ) are represented as shown in Eq. (2). Then,

$$d(A_b)/dt = d[k_1 h(t)\ell(t)]/dt \approx k_1 [h_0 \dot{\tilde{\ell}}(t) + \ell_0 \dot{\tilde{h}}(t)]$$

These parameters are, however, related to fluid that was introduced into the bubble at an earlier time, $t - \tau_0$, where τ_0 is assumed equal to one-half of the bubble mean characteristic time $\ell_{s0}/2|U_c|$, which, in turn, is equivalent to the average convection time over the length of the bubble.

The quasisteady growth relation, Eq. (4), now can be rewritten to reflect the time lag associated with the mass flux term as follows:

$$\begin{aligned} \rho [d(A_b)/dt] &\approx \dot{m}_e(t - \tau_0) \approx \rho 2k_1 E h_0 \dot{\tilde{h}}(t - \tau_0) \\ &\approx \rho k_1 [h_0 \dot{\tilde{\ell}}(t) + \ell_0 \dot{\tilde{h}}(t)] \end{aligned}$$

and we have

$$\dot{\tilde{\ell}}(t) \approx E [2\dot{\tilde{h}}(t - \tau_0) - \dot{\tilde{h}}(t)] \quad (7)$$

Integrating to find the length perturbation, we use $\tilde{h}(t) = \Delta h \cos \omega t$ and assume that over a cycle the average length perturbation is zero, so that

$$\tilde{\ell}(t) \approx E [(2 \cos \omega \tau_0 - 1) \Delta h \cos \omega t + (2 \sin \omega \tau_0) \Delta h \sin \omega t]$$

This can be written as

$$\tilde{\ell}(t) \approx E k_3 \Delta h \cos(\omega t - \gamma) \quad (8)$$

where

$$k_3 = (5 - 4 \cos \omega \tau_0)^{1/2}$$

and

$$\gamma = \tan^{-1} [2 \sin \omega \tau_0 / (2 \cos \omega \tau_0 - 1)]$$

Both k_3 and γ are greater than zero. Note that for quasisteady bubble growth the length perturbation would be given by

$$\tilde{\ell}(t) = E \Delta h \cos \omega t$$

Equation (8) shows that, for relatively low frequencies and small bubbles, such that $\omega \tau_0 < 1$, we have

$$\tilde{\ell}(t) \cong E \Delta h \cos \omega (t - \ell_{s0} / |U_c|)$$

The bubble reattachment point lags its quasisteady location by a time equal to the bubble characteristic time.

In conclusion, it appears that two effects (perturbations to "dead air" pressure and the lag in bubble length) can be extended to the unsteady flow situation from assumptions of quasisteady behavior of the outer shear layer and the finite time lag associated with the convection of mass at a mean velocity in the bubble interior. Comparing unsteady with steady flow separated region behavior, the model predicts a shorter structure with lower surface pressures on the spoiler upstroke, and longer, higher pressure regions on the downstroke. These two features result in unsteady airloads, which can differ significantly from the steady-flow case.

Airfoil with Spoiler/Control Surface Configuration

Aerodynamic loading on a control surface was examined with the purpose of including loading due to spoiler-induced separation in unsteady flow. The spoiler and control surface combination is shown in Fig. 1, and it will be noted that the control surface has a single degree of freedom to rotate about the hinge-line (located at 75% of airfoil chord).

The equation of motion for the control surface may be written as

$$A\ddot{\beta} + B\dot{\beta} + C\beta = H(t)$$

where β is control surface angle, A is the control surface moment of inertia about the hinge-line, B is mechanical damping, and C is structural stiffness. H is the aerodynamic hinge-moment.

Tentatively, it is assumed (with subsequent verification) that the aerodynamic hinge-moment $H(t)$ can be expressed approximately as

$$H(t) \cong H(\beta, \dot{\beta}, h, \dot{h}) \cong H_\beta \beta + H_{\dot{\beta}} \dot{\beta} + \Delta H(h, \dot{h})$$

The equation of motion then can be written as

$$\ddot{\beta} + \frac{(B - H_{\dot{\beta}})}{A} \dot{\beta} + \frac{(C - H_\beta)}{A} \beta = \frac{\Delta H}{A} = \kappa \Delta C_H(h, \dot{h}) \quad (9)$$

The partial derivatives, H_β and $H_{\dot{\beta}}$ are expected to be functions of spoiler amplitude, mean spoiler height, and frequency of oscillation. The dependence of the forcing term ΔC_H on β and $\dot{\beta}$ is neglected at this point.

In steady flow, the hinge-moment coefficient due to a rooftop pressure distribution can be expressed as a polynomial in h

$$\Delta C_H = C_{pb} \sum_{n=0}^{\infty} a_n h^n \quad (10)$$

This representation is found to be valid over a limited, but useful, range of spoiler heights.⁹ Alternatively, the preceding expression can be written in steady flow as

$$\Delta C_H = C_{pb} \sum_{n=0}^{\infty} b_n \ell^n \quad (11)$$

The previous description of unsteady flow modifications to spoiler length and pressures now is introduced in order to approximate the functional form $\Delta C_H(h, \dot{h})$.

Perturbations to pressure at station b in the separated region are assumed to act over the entire forward portion of the region, approximately maintaining the rooftop shape. Lag in bubble length is accounted for also, so that Eq. (11), a steady-flow expression, becomes in unsteady flow

$$\Delta C_H(t) = [C_{pb0} + \tilde{C}_{pb}(t)] \sum_{n=0}^{\infty} b_n [\ell_0 + \tilde{\ell}(t)]^n \quad (12)$$

where C_{pb} and ℓ_0 are constant values, with $\ell_0 = E h_0$. Substituting for \tilde{C}_{pb} from Eq. (6) and for $\tilde{\ell}(t)$ from Eq. (8), we find that the incremental hinge-moment coefficient due to spoiler-induced loading can be written in Fourier series form, since $h(t) = h_0 + \Delta h \cos \omega t$:

$$\Delta C_H(t) = \Delta C_{H0} + \sum_{n=0}^{\infty} \Delta C_{Hn} \cos(n\omega t + \psi_n) \quad (13)$$

The terms ΔC_{H0} , ΔC_{Hn} , and ψ_n are found to be functions of h_0 , Δh , and ω (or ν) by the usual, straightforward method.

In an effort to ascertain the validity of these formulas, an experimental program was conducted as described below.

Description of Experimental Effort

A NACA 0012 airfoil model with one-quarter-chord plain flap and movable fence-type spoiler was constructed and used in a series of tests in the 8 × 6-ft subsonic tunnel at the Cranfield Institute of Technology, England.¹⁰ The spoiler, located at 58.3% chord on the airfoil upper surface, could be oscillated sinusoidally normal to the airfoil chordline over a wide range of mean heights, amplitudes, and frequencies. The airfoil was constructed with a chord c of 24 in. and a span b of 18 in. The control surface extended full span, and its chord c_f was 6 in. Experiments were in the Reynolds number range (based on airfoil chord) of 0.6×10^6 to 2×10^6 .

The model was instrumented with precision miniature pressure transducers located at eight chordwise locations along the centerline. With the control surface fixed, hinge-moments were measured with strain gages. In other experiments, spoiler and control surface motions were measured by precision potentiometers. For fixed spoiler and control surface deflections, shear layer velocity profiles and thicknesses were measured, and surface flow visualization techniques were employed to locate the reattachment point. Cine film recordings of the motion of small tufts provided a means for determining the reattachment location in unsteady flow.

Four configurations were examined initially: 1) control surface and spoiler fixed at various angles or heights (a steady flow situation), 2) control surface fixed and spoiler forced to oscillate sinusoidally, 3) spoiler fixed and control surface forced to oscillate sinusoidally, and 4) control surface free to respond to spoiler-induced loading (spoiler was forced to oscillate). In configuration 4, with the control surface free to oscillate, mechanical stiffness and damping were found to be small compared to aerodynamic contributions. Inertia of the control surface system could be varied between tests. Detailed experimental results can be found in Ref. 10. The following is a summary of some results that served to verify the proposed model.

Results from configuration 1, with the fixed spoiler and control surface, served to confirm steady flow observations mentioned previously and established values for E , the ratio h_0/δ_{r0} , and C_{pb0} . In addition, the validity of Eq. (10) and the constants a_n for $n = 0, 1, 2, 3, 4, 5$ were found. It also was found that a fifth-order polynomial in h provided an appropriate approximate representation for $\Delta C_H(h)$.

Results from configuration 2, with the control surface fixed and the spoiler forced to oscillate, established that Eqs. (12) and (13) are reasonable approximations, as shown in Fig. 4. The three unsteady cases shown involve different values of h_0 and Δh but a constant reduced frequency ν . The solid,

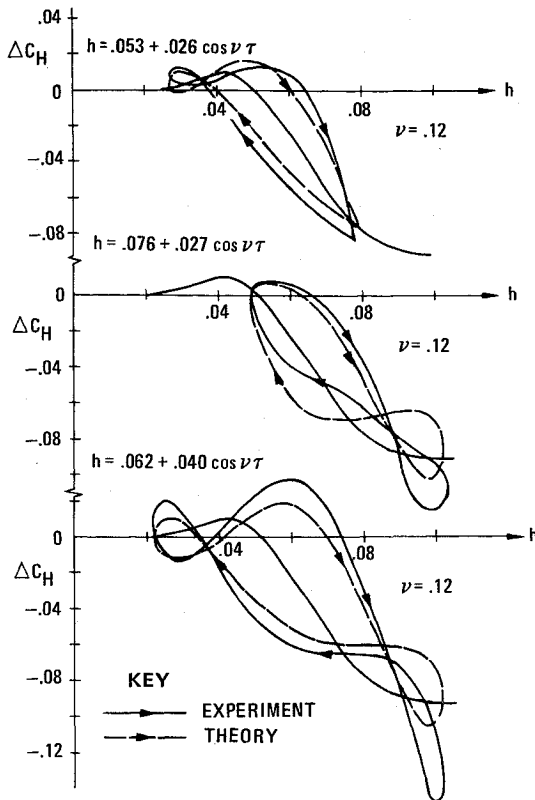


Fig. 4 Dynamic hinge moment variations.

single-valued curve (common to each set of curves) is the nonlinear steady flow relation given by Eq. (10). Theoretical predictions of $\Delta C_H(t)$ are seen to compare with experiment with fair accuracy even in these cases of relatively large perturbations.

Results from configuration 3, with the spoiler fixed and the control surface forced to oscillate, served to establish values of $H_\beta(h_0, \nu)$ and $H_\beta(h_0, \nu)$. These partial derivatives were found to be insensitive to control surface amplitude of oscillation up to amplitudes of about 10 degrees. Furthermore, the derivatives are found to be very weakly dependent on spoiler height for low-to-moderate values of h_0 . This range of spoiler heights relates to separation regions of a size such that reattachment or significant recompression occurs on the control surface. As Maskell¹¹ points out, in such cases the control surface is able to "control" the flowfield much as it does for attached flow. It also was noted that H_β and H_β are weak functions of frequency over the relatively low values of which are of interest. Thus, in Eq. (9), we use

$$H_\beta = C_{H_\beta} q_\infty b c_f^2$$

and

$$H_\beta = C_{H_\beta} (c_f/U_\infty) q_\infty b c_f^2$$

where the nondimensional derivatives C_{H_β} and C_{H_β} are approximated by empirical constants.

Results from configuration 4, with the control surface free to respond to spoiler-induced loading, confirmed the validity of the equation of motion, Eq. (9). When the spoiler is oscillated in simple harmonic motion, the forcing function $\Delta C_H(h_0, \Delta h, \nu)$, which contains higher harmonic components of the fundamental frequency, causes the control surface to oscillate so that the steady-state response $\beta(t)$ can be written as

$$\beta(t) = \beta_0 + \sum_{n=1}^{\infty} \beta_n \cos(n\omega t + \phi_n) \quad (14)$$

In the experiment, values of β_0, β_n , and ϕ_n for $n = 1, 2, 3, 4$ were measured and compared to those predicted by Eq. (9) with good results.¹⁰ Forcing functions used in solutions of Eq. (9) were determined from experimental results with the control surface fixed (configuration 2).

We can, therefore, assume that the proposed expression for the aerodynamic hinge-moment preceding Eq. (9) is a reasonable approximation. In particular, the effects of control surface angle and rate on the component representing spoiler-induced loading are seen to be negligible. Furthermore, the formulation of aerodynamic hinge-moment employing a superposition of the contributions from the control surface and spoiler is observed to be appropriate.

Analysis of Coupled System Behavior

One final experimental configuration involved the mechanical coupling of the control surface to the spoiler so that spoiler motion was related directly to control surface motion through the coupling equation

$$h = h_{01} + k\beta \quad (15)$$

where h_{01} and k are parameters that were held constant during an experiment. The aerodynamic coupling described earlier must, of course, be considered also.

This kind of mechanical coupling has been investigated experimentally by Phillips and Adams,¹² who employed a somewhat similar apparatus which involved an airfoil control surface and two spoilers; one on the upper and one on the lower surface. They observed self-excited behavior, which led to limit-cycle oscillations for a critical value of mean spoiler height, but such behavior was restricted to a fairly narrow range of freestream speeds. This phenomenon is thought to be a subsonic analogy of transonic control surface buzz, where unsteady separation is induced by shock-wave motion. The behavior of such a coupled system is examined below.

Steady flow solutions to Eq. (9), found in the absence of motion, lead to a value of β such that

$$[(C - H_\beta)/A]\beta = \kappa \Delta C_H(h_0)$$

Since spoiler height and control surface angle are related through Eq. (15), this can be rewritten as

$$\beta = [A/(C - H_\beta)]\kappa \Delta C_H(\beta) \quad (16)$$

However, we can expect that the unsteady loading due to spoiler motion, which lags control surface motion for the coupled system, may result in self-excitation over a critical range of h_{01} and k . Oscillations of increasing amplitude may result until a limit-cycle oscillation of constant amplitude is reached. Such a possibility was demonstrated in the Phillips and Adams experiment¹² and will be considered now.

Use of the mechanical coupling relation [Eq. (15)] leads to a slightly altered unsteady flow formulation of system behavior:

$$\beta + \frac{(B - H_\beta)}{A} \dot{\beta} + \frac{(C - H_\beta)}{A} \beta = \kappa \Delta C_H(\beta, \dot{\beta}) \quad (17)$$

The left-hand side of this relation is observed to represent a system with low pass filter characteristics. Thus, the motion of the coupled autonomous system is expected to be nearly sinusoidal, a characteristic that has been observed.¹² Approximate solutions to Eq. (17) then are expected to take the form

$$\beta(t) = \beta_0(t) + \Delta\beta(t) \cos[\omega(t) \cdot t] \quad (18)$$

Time dependence of the center of oscillation β_0 can be expected, since the spoiler is located only on the airfoil upper surface. This flow asymmetry is somewhat analogous to that due to airfoil incidence in the transonic "buzz" example.

From Eq. (15) and (18), we find that control surface motion is related to that of the spoiler such that

$$h(t) = h_0(t) + \Delta h(t) \cos[\omega(t) \cdot t]$$

where

$$h_0(t) = h_{0i} + k \beta_0(t)$$

and

$$\Delta h(t) = k \Delta \beta(t)$$

A complete solution of Eq. (17) will not be attempted. However, the parameters β_0 , $\Delta \beta$, ω , and λ will be investigated for two critical cases: 1) the system is at a nominal equilibrium position given by a solution of Eq. (16) with $\Delta \beta = 0$; and 2) the system has achieved a limit-cycle oscillation where amplitude is constant and $\lambda = 0$.

Extension of the method of Beecham and Titchener¹³ to this asymmetric flow configuration results in algebraic equations⁹ for the parameters β_0 , λ , and ω^2 :

$$\beta_0 \cong \frac{\Delta C_{H_0}}{[(C/q_\infty b c_f^2) - C_{H_\beta}]} \quad (19a)$$

$$\lambda \cong \frac{1}{2A} \left[\left(\frac{c_f}{U_\infty} C_{H_\beta} + k \frac{N_2}{\omega} \right) q_\infty b c_f^2 - B \right] \quad (19b)$$

$$\omega^2 \cong -\lambda^2 + \left[\frac{C - (C_{H_\beta} + k N_1) q_\infty b c_f^2}{A} \right] \quad (19c)$$

In the preceding formulation, the parameters $\beta_0(t)$, $\Delta \beta(t)$, $\omega(t)$, and $\lambda(t)$ are assumed to vary slowly with time and can, therefore, be represented by average values taken over a cycle of oscillation. The quantities ΔC_{H_0} , N_1 , and N_2 are termed "describing functions." They are evaluated analytically, using the postulated function $\Delta C_H(h, \dot{h})$ according to the following formulas¹⁴

$$\Delta C_{H_0}(h_0, \Delta h, \omega) = \frac{1}{2\pi} \int_0^{2\pi} \Delta C_H(h_0, \Delta h, \omega) d(\omega t) \quad (20a)$$

$$\begin{bmatrix} N_1(h_0, \Delta h, \omega) \\ N_2(h_0, \Delta h, \omega) \end{bmatrix} = \frac{1}{\pi \Delta h} \int_0^{2\pi} \Delta C_H(h_0, \Delta h, \omega) \begin{bmatrix} \cos \omega t \\ \sin \omega t \end{bmatrix} d(\omega t) \quad (20b)$$

The resultant describing functions are general in that they may be used to study system stability, and transient or steady-state (e.g., limit-cycle) behavior. They represent contributions to terms in a Fourier series for ΔC_H , e.g.,¹⁴

$$\Delta C_H \cong \Delta C_{H_0} + \left[N_1 + \frac{N_2}{\omega} \lambda \right] k \Delta \beta \cos \omega t + \frac{N_2}{\omega} (-\omega k \Delta \beta \sin \omega t) + \dots$$

Complete expressions are found in Ref. 9.

First, the system is taken to be at rest at the steady-flow equilibrium position given by Eq. (16). At this point, $\Delta \beta = \Delta h = 0$. The coupling parameters, h_{0i} and k , were varied over a wide range, and an iterative computational scheme was used in order to find solutions to the set of equations (19). Figure 5 shows predicted curves of constant β_0 , λ , and ν for the configuration, assuming ideal coupling. "Ideal" implies that dry friction, which existed in the experimental apparatus and prevented self-excited oscillations, was not included. The curve representing $\lambda = 0$ defines the system stability boundary. The stable region is confined roughly to the left side of the graph, where the combination of mechanical damping and the aerodynamic contribution due to H_β is greater in magnitude than the negative damping due to the unsteady bubble. Lines of constant center of oscillation β_0 are straight. For any given k , the system is most unstable for $h_{0i} \cong 0.065$, which corresponds to $\beta_0 \cong -4^\circ$. It is shown in Refs. 9 and 10 that this "critical" spoiler height approximately coincides with a separation bubble of such length that reattachment occurs at the trailing edge. The magnitudes of N_1 and N_2 are greatest (for $\Delta h \cong 0$) at this height.

Secondly, limit-cycle behavior was investigated again for the case of ideal mechanical coupling by use of Eqs. (19) with

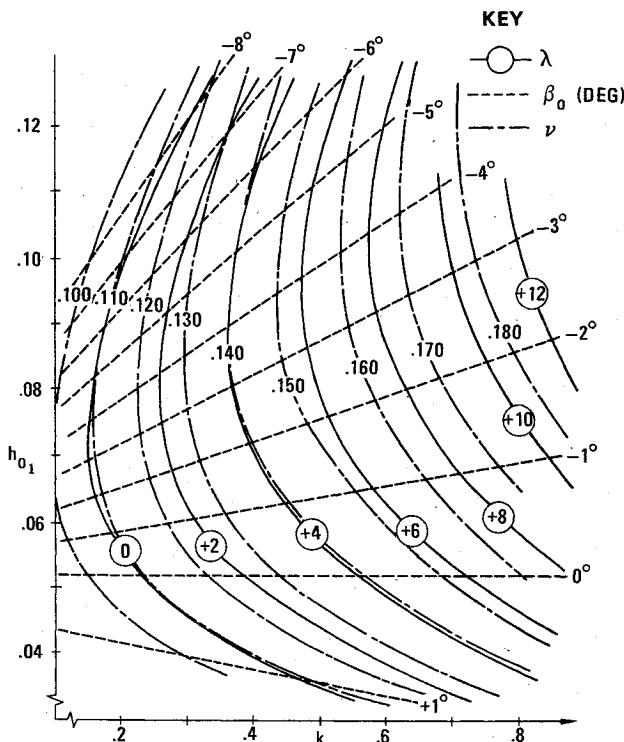


Fig. 5 Predicted stability map for the mechanically coupled system.

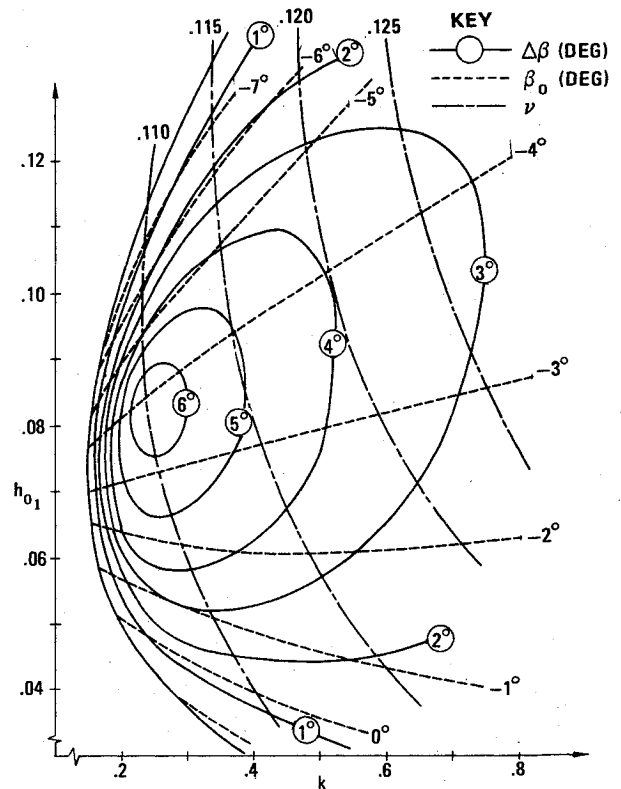


Fig. 6 Predicted limit cycle behavior: ideal (frictionless) coupling.

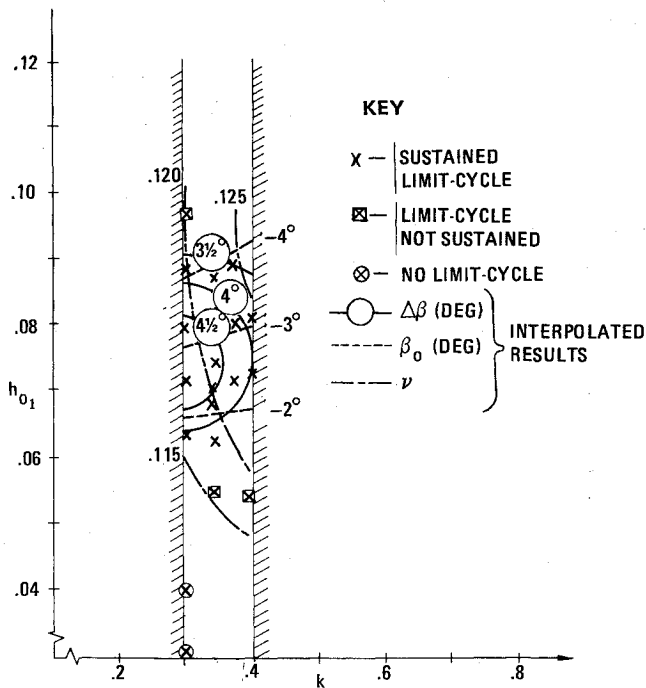


Fig. 7 Limit cycle parameters: experimental values.

$\lambda=0$. Stability analysis confirms that the limit cycles are stable.⁹ Figure 6 contains curves of constant β_0 , $\Delta\beta$, and ν for the limit cycle condition. These curves, when compared to those of Fig. 5, lead to the following conclusions:

1) The curve of $\Delta\beta=0$ defines the limit-cycle region and nearly coincides with the neutral stability curve of Fig. 5. Hence, what is termed soft oscillator excitation is predicted for a wide range of h_{01} and k values where $\lambda>0$. For very low values of h_{01} and k , the hard oscillator condition exists; i.e., it appears that a substantial initial condition is needed to cause limit-cycle behavior.

2) Maximum amplitude limit-cycle behavior is associated with the "critical" spoiler height and an intermediate value of k . For lower k values, mechanical damping dominates. For higher values of this parameter, the frequency is high, and the amplitude is correspondingly low.

3) Curves of constant β_0 are not straight lines due to a so-called "rectification effect" on ΔC_{H_0} , which results from the dependence of spoiler-induced loading on amplitude and frequency.

4) For given values of h_{01} and k , reduced frequency is lowest in the limit-cycle case, since system stiffness decreases with increasing amplitude.

To compare theoretical predictions with experiment, curves of constant β_0 , $\Delta\beta$, and ν were interpolated from numerous experimental observations that involved different values of h_{01} and k . The data are presented in Fig. 7. The range of k values was confined to a narrow band because of mechanical limitations of the apparatus. Center of oscillation, amplitude, and frequency data are within 20% of values based on the curves. The effect of dry friction required a fairly large initial flap displacement to achieve limit-cycle behavior.

The analytical predictions, which include an experimentally verified model for the dry friction, are shown in Fig. 8. The shaded region indicates where convergence of the iterative computational scheme was not achieved. The predictions are observed to compare favorably with the experimental results, especially in the region of maximum amplitudes where h_0 is near the "critical" value. Larger values of h_0 (hence h_{01}) correspond to longer separation bubbles, where recompression occurs in the wake as well as on the flap upper surface. The mass flux and pressure perturbation features of the model are not expected to be applicable in this case.

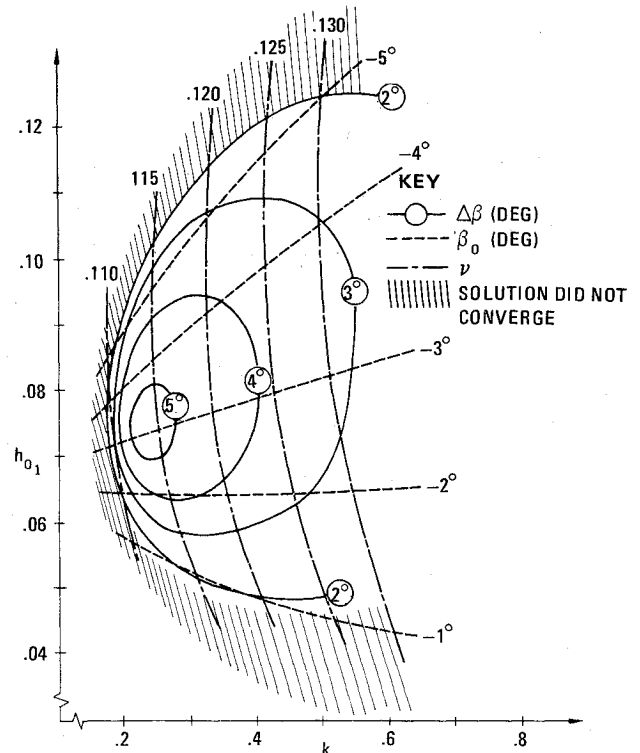


Fig. 8 Predicted limit cycle behavior: dry friction included.

It appears that a critical degree of mean separation and a moderate amount of coupling between flap and spoiler motion is necessary in order to achieve maximum-amplitude limit cycles. This conclusion may relate to analogous dependence of actual control-surface buzz on a critical degree of separation (e.g., due to angle of attack, thickness, and Mach number) and a reduced frequency range.

Conclusions

The viability of the proposed model for separation "bubble" behavior in the unsteady case is guaranteed somewhat by the fact that its foundation is predicated on physical characteristics that have been derived from experimental observation. It is, therefore, no surprise that the application of the resultant analytical formulation to the particular configuration involving a mechanically coupled spoiler and control surface should lead to satisfactory agreement with the experimental simulation.

The self-excited oscillations and resultant limit-cycle behavior are unique features of the configuration which allow limited analogy with transonic control-surface buzz. Because of their functional relationship in the system equation of motion, the features of bubble growth lag and the resultant pressure field modifications may be viewed as the primary physical drive for this behavior.

For the sake of completeness, however, other elements of the actual physical situation must be incorporated to provide a more accurate model capable of describing shear layer conditions. The role of turbulent shear stresses and their significance in vorticity production and transfer should be examined, along with considerations of the "bubble" geometry. Three-dimensional mean flow characteristics within the bubble also must be investigated to ascertain their role in the overall development of the dynamics of this region.

References

- Chang, P.K., *Separation of Flow*, 1st ed., Pergamon Press, London, 1970.
- Crimi, P. and Reeves, B.L., "A Method for Analyzing Dynamic Stall of Helicopter Rotor Blades," NASA CR-2009, May 1972.

³Newman, B.G., "The Re-Attachment of a Turbulent Boundary-Layer Behind a Spoiler," Aero Research Labs., Melbourne, Australia, Rept. A64, 1949.

⁴Norbury, J.F. and Crabtree, L.F., "A Simplified Model of the Incompressible Flow Past Two-Dimensional Aerofoils with a Long Bubble Type of Flow Separation," Royal Aircraft Establishment, England, Tech. Note Aero 2352, June 1955.

⁵Horton, H.P., "A Semi-Empirical Theory for the Growth and Bursting of Laminar Separation Bubbles," Current Paper 1073, June 1967, Aeronautical Research Council.

⁶Trilling, L., "Oscillating Shock Boundary-Layer Interaction," *Journal of the Aeronautical Sciences*, Vol. 25, May 1958, pp. 301-304.

⁷Barnes, C.S., "Two-Dimensional Normal Fences on a Flat Plate," Current Paper 863, Feb. 1965, Aeronautical Research Council.

⁸East, R.A. and Wilkinson, P.R., "A Study of the Oscillating Laminar Separated Flow Ahead of a Forward Facing Step Oscillating

Transversely to a Hypersonic Free Stream," *Separated Flows, Part 2, AGARD Conference Proceedings No. 4*, May 1966, pp. 509-530.

⁹Lang, J.D., "The Dynamics of a Growing Separated Region on an Airfoil," USAF Academy, F.J. Seiler Research Lab TR-75-0005, (AD-A008773), Feb. 1975.

¹⁰Lang, J.D., "Experiments on an Airfoil with Oscillating Spoiler and Flap," USAF Academy, F.J. Seiler Research Lab. TR-74-001, (AD-783251), June 1974.

¹¹Maskell, E.C., "Pressure Distributions Illustrating Flow Reattachment Behind a Forward Mounted Flap," Current Paper 211, March 1954, Aeronautical Research Council.

¹²Phillips, W.H. and Adams, J., "Low-Speed Tests of a Model Simulating the Phenomenon of Control Surface Buzz," NACA/RM L50F19, 1950.

¹³Beecham, L.J. and Titchener, I.M., "Some Notes on an Approximate Solution for the Free Oscillation Characteristics of Nonlinear Systems Typified by $\ddot{x} + F(x, \dot{x}) = 0$," ARC R&M 3651, 1971, Aeronautical Research Council.

¹⁴Siljak, D.D., *Nonlinear Systems*, Wiley, New York, 1969.

From the AIAA Progress in Astronautics and Aeronautics Series . . .

AEROACOUSTICS: JET AND COMBUSTION NOISE; DUCT ACOUSTICS—v. 37

Edited by Henry T. Nagamatsu, General Electric Research and Development Center; Jack V. O'Keefe, The Boeing Company; and Ira R. Schwartz, NASA Ames Research Center

A companion to Aeroacoustics: Fan, STOL, and Boundary Layer Noise; Sonic Boom; Aeroacoustic Instrumentation, volume 38 in the series.

This volume includes twenty-eight papers covering jet noise, combustion and core engine noise, and duct acoustics, with summaries of panel discussions. The papers on jet noise include theory and applications, jet noise formulation, sound distribution, acoustic radiation refraction, temperature effects, jets and suppressor characteristics, jets as acoustic shields, and acoustics of swirling jets.

Papers on combustion and core-generated noise cover both theory and practice, examining ducted combustion, open flames, and some early results of core noise studies.

Studies of duct acoustics discuss cross section variations and sheared flow, radiation in and from lined shear flow, helical flow interactions, emission from aircraft ducts, plane wave propagation in a variable area duct, nozzle wave propagation, mean flow in a lined duct, nonuniform waveguide propagation, flow noise in turbofans, annular duct phenomena, freestream turbulent acoustics, and vortex shedding in cavities.

541 pp., 6 x 9, illus. \$19.00 Mem. \$30.00 List

TO ORDER WRITE: Publications Dept., AIAA, 1290 Avenue of the Americas, New York, N. Y. 10019